J Mater Sci: Mater Electron
DOI 10.1007/s10854-013-1568-5

Influence of zirconium addition on final properties of $K_{0.5}Na_{0.5}NbO_3$-based ceramics

L. Ramajo · J. Taub · M. S. Castro

Received: 16 August 2013 / Accepted: 22 October 2013
© Springer Science+Business Media New York 2013

Abstract Microstructure, electrical and dielectric properties of $K_{1/2}Na_{1/2}NbO_3$ (KNN) modified with ZrO_2 were investigated. Powders were obtained by a conventional solid-state method. Samples doped with 0–2 mol% of ZrO_2 were sintered at 1,125 °C for 2 h. Through XRD spectra, the perovskite structure was observed, in addition to small peaks corresponding to secondary phases. It was also determined that zirconium drastically changed the microstructure and grain size of KNN ceramics. The addition of upto 1.0 mol% of Zr^{4+} produced a softening effect in the ferroelectric properties of the material, and increased its density. Conversely, samples prepared with contents higher than 1.0 mol% reduced piezoelectric and dielectric properties.

1 Introduction

Piezoelectric ceramics have important roles in electromechanical and electronic devices such as actuators, generators, transducers and sensors. The most important and widely used piezoelectric compositions are lead zirconate titanate (PZT) based ceramics [1–3]. However, PZT ceramics contain more than 60 wt% of lead which, making them a serious threat to human health and the environment. This is especially important during the sintering process where vapor pressure containing lead compounds is built. Consequently, lead-free piezoelectric ceramics have attracted great attention over the past few years [4–6].

Numerous studies on lead-free piezoelectric ceramics have been published [7–10]. Environmentally friendly niobates, such as $(K,Na)NbO_3$-based ceramics, have shown valuable piezoelectric and electric properties when the compositional ratio of K/Na is near 50/50. This composition is reported to show a virtual morphotropic phase boundary where the total polarization is maximized by an increase in oriented domains. Nevertheless, the dielectric and piezoelectric properties of pure KNN are relatively low ($d_{33} \sim 90$ pC/N) as compared to those achieved with PZT. This makes the replacement of conventional PZT with KNN very difficult [11–14].

Previous works have shown that the addition of low contents of zirconium oxide KNN phase hinders the grain growth of $K_{0.5}Na_{0.5}NbO_3$ ceramics during sintering in air [15]. This refinement on the microstructure was attributed to two processes. Firstly, zirconia particles located at the matrix grain junctions decrease the mobility of the matrix grain boundaries. Secondly, a greater enrichment has been detected in the region of the grain boundaries relative to the grain interior, due to a limited solubility of zirconium in the perovskite network. This enrichment in zirconium was explained by the diffusion of zirconium in the perovskite lattice. According to the ionic radius and coordination chemistry of Zr and Nb ions, a limited solid solubility of Zr in $K_{0.5}Na_{0.5}NbO_3$ with Zr^{4+} occupying the Nb^{5+} sites in the perovskite lattice could be expected. Consequently, vacancies should be formed in the O-sublattice. This defect structure of the grain boundary regions may also limit their mobility during the sintering process [15–17]. Other studies have shown that the densification is improved by ZrO_2 doping, but does not prevent the

L. Ramajo (✉) · J. Taub · M. S. Castro
Instituto de Investigaciones en Ciencia y Tecnología de Materiales (INTEMA), CONICET-UNMdP, J. B. Justo 4302, B7608FDQ Mar del Plata, Argentina
e-mail: lramajo@fi.mdp.edu.ar

Published online: 08 November 2013

evaporation of alkali elements for high sintering temperature [18].

In this work, the structural and microstructural evolution and its reflection on the final properties of the ceramic obtained with the addition of zirconium oxide is presented. Different contents of Zr^{4+} incorporated during the formation of the $K_{0.5}Na_{0.5}NbO_3$ phase were analyzed to provide an alternative approach for lead-free materials development.

2 Experimental

Lead-free potassium sodium niobate $K_{0.5}Na_{0.5}NbO_3$ (KNN) modified with Zr^{4+} was produced by the conventional solid state reaction method from potassium carbonate (Biopack 99.5 %, Argentina), sodium carbonate (BioPack 99.5 %, Argentina), niobium oxide (Aldrich 99.9 %, USA), and zirconium oxide (Anedra, 99.0 % Argentina). Powders with K: Na = 1:1, and different Zr^{4+} concentrations (x = 0, 0.5, 1 and 2 mol%) were mixed in 2-propanol and milled in a planetary laboratory ball-mill (Fritsch, Pulverisette 5), with zirconium oxide grinding jars and balls, for 6 h at 1,000 rpm. Afterwards, the resulting powders were calcined at 900 °C for 5 h in air.

The resulting powders were uniaxially pressed into discs of 6 mm diameter and 0.5 mm thick. In order to analyze the influence of zirconia addition on KNN-ceramics, all samples were sintered using the same sintering cycle (1,125 °C for 2 h in a conventional furnace using 5 °C/min heating and cooling rates).

The crystalline phases were assessed by X-ray diffraction, employing a Philips PW1050/25 diffractometer running with CuK_α radiation, at 40 kV and 30 mA. The microstructure of the samples was examined by Scanning Electron Microscopy (SEM), using a JEOL JSM-6460LV microscope. Raman spectra were acquired at room temperature with a Renishaw inVia Raman spectrometer by means of the 514 nm Ar-ion laser line (10 mW nominal power).

For the electrical measurements, silver electrodes were painted on both faces of the sintered samples. Dielectric properties were measured using a frequency range of 0.10 Hz–10 MHz, employing both Hioki 3,535 and 3,522–50 LCR meters. Polarization versus electric field hysteresis loops were obtained in a silicone oil bath at room temperature by applying an electric field of sinusoidal waveform at a frequency of 50 Hz by means of a modified Sawyer–Tower bridge. For the measurement of the piezoelectric constant, samples were first polarized inside a silicone oil bath using 2.5 kV/mm for 30 min at 150 °C, and finally, the piezoelectric coefficients d_{33} were recorded using a quasi-static piezoelectric d_{33} meter (Piezo d33 Test System Model: YE2730-Sinocera Inc.).

3 Results and discussion

Figure 1 shows XRD spectra corresponding to KNN-based ceramics doped with different zirconium amounts (0–2 mol%). The presence of a predominant phase associated to KNN perovskite structure has been detected. As expected, coexistence of the orthorhombic-tetragonal phase was observed. Interestingly, when the Zr^{+4} content is $\leq$1.0 mol%, the prepared samples were orthorhombic specified by the splitting of the (022) and (200) reflections and by higher intensity counts for the (022) peaks. Further increase in the Zr^{+4} concentration reduces the splitting of (022) and (200) orthorhombic reflections. This indicates that the dopant is incorporated into the perovskite structure and, on the other hand, it forms a significant amount of tetragonal phase at 2 mol%. This tendence was also confirmed in the diffraction peaks located at a higher angle (Fig. 2). Moreover, small peaks related to the presence of a secondary phase can be assigned to $K_4Nb_6O_{17}$ (JCPDS 76-0977) resulting from slight changes in stoichiometric ratio due to highly volatile alkaline elements during sintering process. Zirconium addition promotes the apparition of this secondary phase, associated to the incorporation of this additive in the perovskite structure. Through this technique, the presence of ZrO_2 particles was not detected, probably because they were below the detection limit.

The Raman spectra of the KNN samples doped with zirconium are shown in Fig. 3. This spectroscopic technique is a very sensitive tool to study the structural deformations of the ceramic unit cell at a local scale. In the KNN structures, the main vibrations are associated with the NbO_6^- octahedron (BO_6^-) [19]. Therefore, the deformations are induced by the tilting of octahedral and the cationic displacements

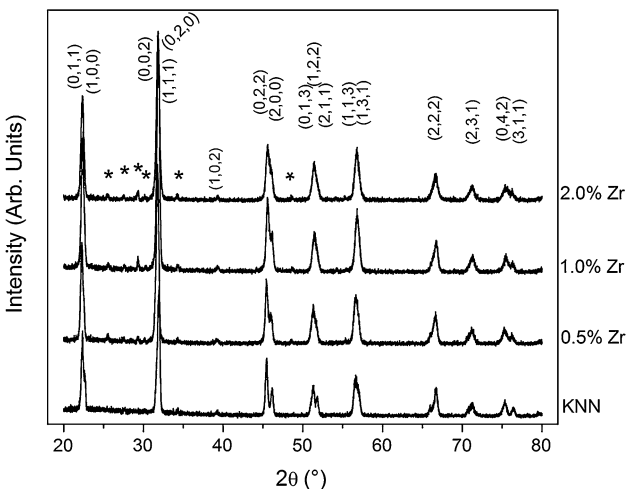

Fig. 1 XRD patterns of pure and zirconium-doped KNN ceramic (JCPDS 71-1098). (*) Signals corresponding to $K_4Nb_6O_{17}$ (JCPDS 76-0977)

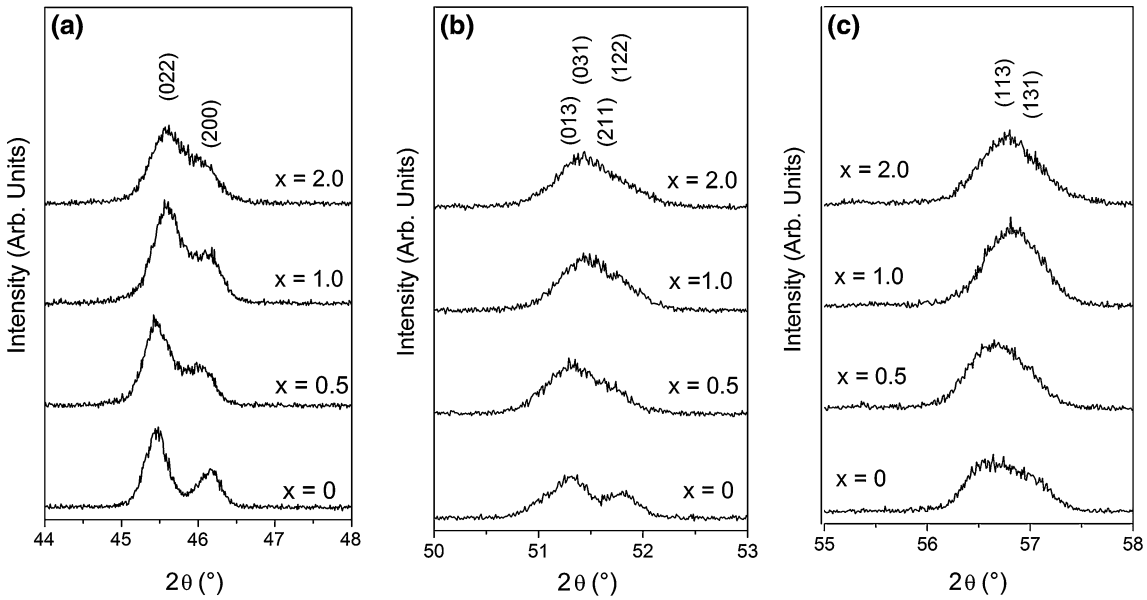

Fig. 2 XRD magnified patterns in the 44–48° (**a**), 50–53° (**b**), and 55–58° (**c**) 2θ range

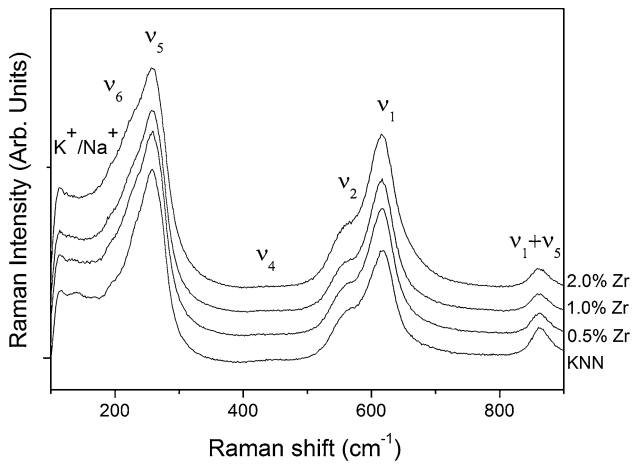

Fig. 3 Raman spectra corresponding to pure KNN and KNN doped with several zirconium amounts (0.5–2 mol%)

[20]. These modifications induce large changes in internal modes associated with NbO_6^- octahedron resulting in a modification of the Raman spectra [21]. Therefore, it can be appreciated that the Raman spectrum peaks related to the vibrations of the NbO_6^- octahedron consist of $A_{1g}(\upsilon_1) + Eg(\upsilon_2) + F_{1u}(\upsilon_3, \upsilon_4) + F_{2g}(\upsilon_5) + F_{2u}(\upsilon_6)$. Vibrations modes $A_{1g}(\upsilon_1) + E_g(\upsilon_2) + F_{1u}(\upsilon_3)$ are stretching modes, and the rest of them are bending modes. In particular, $A_{1g}(\upsilon_1)$ and $F_{2g}(\upsilon_5)$ have been detected as being relatively strong scatterings in similar systems to the one studied in this work due to a near-perfect equilateral octahedral symmetry. Finally, the peaks in the region between 100 and 160 cm^{-1} can be associated with translational models of alkaline niobates K^+/Na^+ and rotational modes of the NbO_6^- octahedron [22, 23].

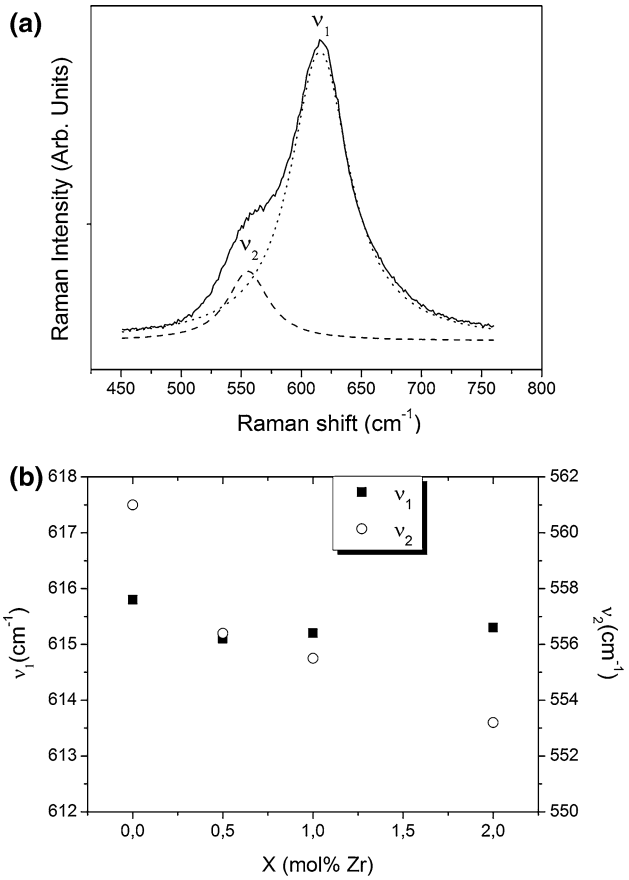

Fig. 4 Magnification of the Raman spectra in the 450–760 cm^{-1} range. *Dotted lines* represent the Gaussian adjustment of the individual bands of A_{1g} (υ_1) and E_g (υ_2) Raman modes (**a**). υ_1 and υ_2 Raman modes values obtained after fitting as a function of zirconium concentration (**b**)

Figure 4a shows representative enlarged Raman spectra of pure KNN between 450 and 760 cm^{-1}. The adjustment to the sum of two Gaussians ascribed to υ_2 and υ_1 Raman modes, respectively, is also shown. In Fig. 4b it can be seen that the value of υ_1 is practically constant even if the amount of the additive is higher. However, the value of υ_2 decreases when the zirconium concentration increases. This observation can be related to modifications in the stabilized perovskite structure. Indeed, in the orthorhombic phase there is a distinct shoulder in the Raman spectra on the low-frequency side of the main Raman mode (υ_1), this shoulder is also present in the tetragonal phase although rather weaker [19].

Figure 5 shows Scanning Electron Microscopy images of the sintered samples. Samples composed of pure KNN present cubic grains with a bimodal grain size ($\sim$3 and $\sim$1 μm). Ceramics with the lowest zirconium addition (0.5 mol%) developed a fine microstructure with an average grain size close to 1 μm, as well as, the formation of a glassy phase. It has been observed that, the higher the additive amount, the higher the glassy phase. Finally, in samples with the highest additive amount (2 mol%) a slight increase in the grain growth and in the glassy phase amount have been observed. According to the phase diagram the niobium excess forms a liquid at 1,058 °C that could promote sintering with grain coarsening without exaggerated grain growth [21, 23]. Furthermore, the appearance of the secondary phase is associated with the transitory liquid phase that assisted the sintering process. Moreover, as the amount of zirconium increases, niobium is replaced in the perovskite lattice and, consequently, the transient liquid phase and niobium-rich secondary phases are promoted.

The grain refinement may be associated with ZrO_2 inclusions that hinder the grain growth [16, 17]. A similar

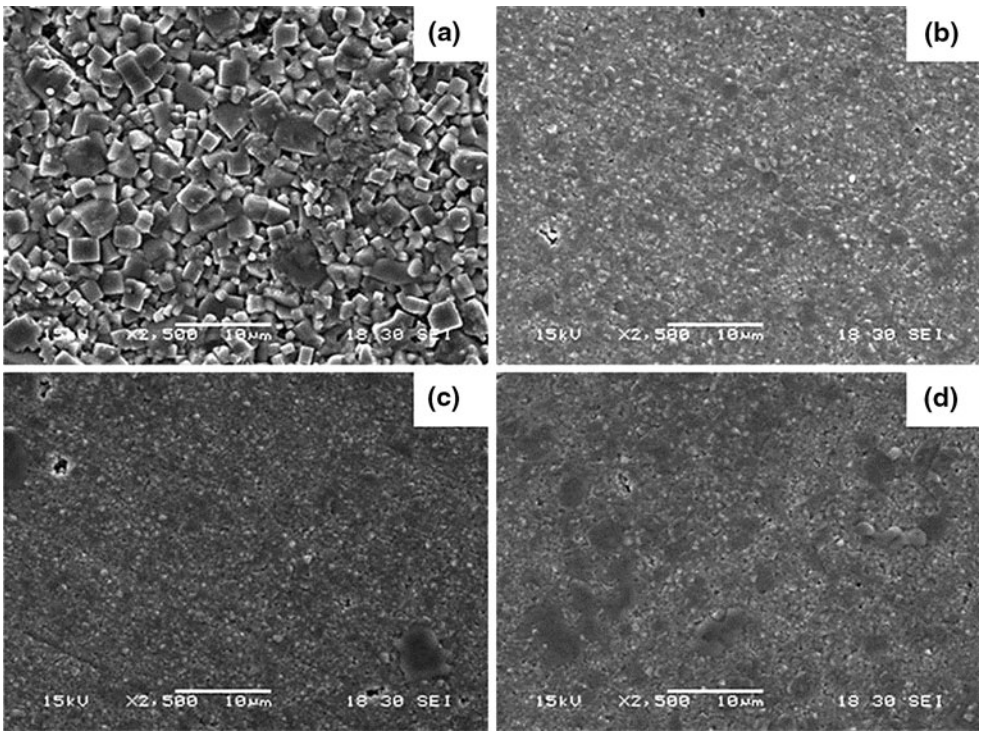

Fig. 5 SEM images of pure KNN (**a**) and KNN doped with 0.5 mol% (**b**), 1 mol% (**c**) and 2 mol% of zirconium (**d**)

Table 1 Density and porosity values, as well as, dielectric and piezoelectric properties of the studied samples

Sample	Density (g/cm^3)	Porosity (%)	ε' (10 kHz)	tanδ (10 kHz)	d_{33} (pC/N)
Pure KNN	4.28 ± 0.19	5.75 ± 2.45	352	0.13	86
KNN 0.5 mol %Zr	4.37 ± 0.01	3.28 ± 0.31	452	0.065	115
KNN 1.0 mol %Zr	4.41 ± 0.06	2.12 ± 1.34	450	0.076	108
KNN 2.0 mol %Zr	4.32 ± 0.086	4.58 ± 2.09	458	0.070	73

Theorical density 4.51 g/cm^3

influence on the microstructure was also found by Malic et al. [15] when ZrO_2 powder was added to the KNN synthesized powder.

In Table 1, density values of sintered samples have been presented. According to this table, there is an improvement in density values with the additive incorporation. This behavior can be attributed to the small grain growth and the formation of the glassy phase.

Figure 6 shows real permittivity and loss tangent values as a function of frequency for samples with different additive amounts. In all cases, it can be seen that at low frequency, permittivity decreases drastically with frequency due to a space charge relaxation process characteristic of the polycrystalline material. Additionally, a relaxation process at high frequency (~5 MHz) which is associated with a dipolar relaxation phenomena can be observed. In these samples, the addition of zirconium oxide causes an increase in real permittivity due to a good densification.

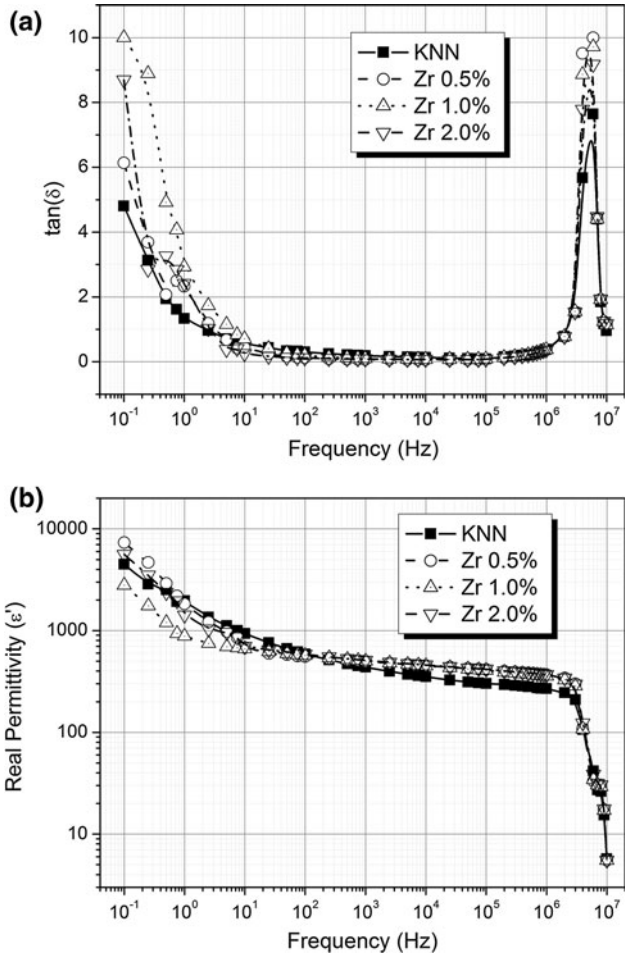

Fig. 6 Curves of loss tangent (**a**) and real permittivity (**b**) as a function of frequency at room temperature

Table 1 also shows values of real permittivity (ε'), loss tangent (tanδ) and piezoelectric constant (d_{33}) corresponding to KNN with different zirconium amounts (0–2 mol%). From these values, it can be observed that the incorporation of this additive improves the dielectric properties of the device, increasing the real permittivity and decreasing the loss tangent. Moreover, an improvement in the piezoelectric constant value with the lowest percentage of zirconium was found. These enhanced properties are associated with the higher density values obtained with the ZrO_2 addition, using the same sintering cycle.

Figure 7 presents the hysteresis loops at room temperature of sintered samples. Pure KNN samples show a remnant polarization (P_r) 13.75 μC/cm^2, which is greater than the Zr-doped samples with 6.43; 5.85 and 8.19 μC/cm^2 for samples with 0.5, 1 and 2 mol% Zr, respectively. The coercive electric field (E_c), and the saturation polarization values (P_s), for the doped samples with 0–2 mol% Zr, were 17.3, 12.0, 11.32, 11.92 kV/cm and 18, 25, 12.87, 11.70 and 14.05 μC/cm^2, respectively.

From the decrease in the coercive electric field value, a softening effect on the ferroelectric properties of KNN with zirconium addition was detected. This result cannot be related to the possible Zr^{4+} substitution in Nb^{5+} positions of the lattice with the consequent oxygen vacancy generation, which produces a hardening effect on the ferroelectric properties of the material. In this case, the increased material density strongly modified the final behavior of these devices. The diminution in the sample porosity facilitates the movement of the dipoles and, consequently, reduces electrical losses.

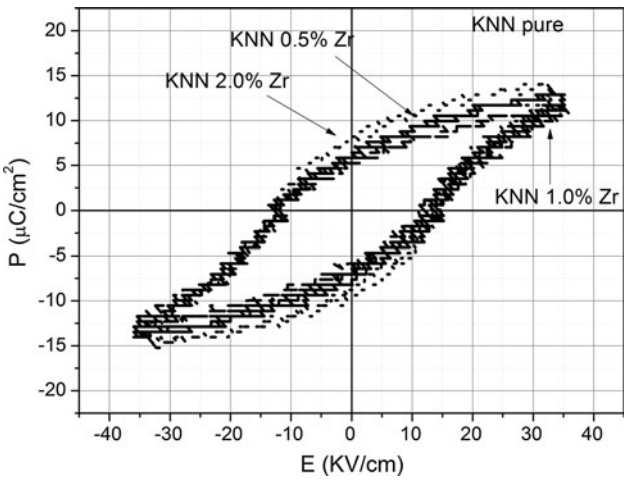

Fig. 7 Hysteresis loops of sintered samples. Measuring conditions: room temperature, *ac* field, electric field of 35 kV/cm and frequency of 50 Hz

4 Conclusions

The effect of ZrO_2 on KNN added before calcination at different concentrations is studied. It was found that some Zr^{4+} ions replace Nb^{5+} ions in "B" positions of the perovskite lattice, while ZrO_2 particles could be located at the grain boundaries. The latter effect hinders grain growth, improving the packing, thus increasing the final density of the sample. With the rise in doping concentration the replacement in B positions is increased and the formation of a glassy phase is observed. Increased density was shown to improve the dielectric and piezoelectric properties of the material. From the balance between density and the amount of secondary phases, it is concluded that the best properties are obtained with the lowest zirconium concentrations tested in this work (0.5 mol%).

Acknowledgments This work was supported by Consejo Nacional de Investigaciones Científicas y Técnicas (CONICET), Agencia Nacional de Promoción Científica y Tecnológica (ANPCyT) and Universidad Nacional de Mar del Plata (UNMdP), Argentina. Also, L'Oréal—UNESCO "For Women in Science" Program is acknowledged.

References

1. T.R. Shrout, S. Zhang, J. Electroceram. **19**, 113–116 (2007)
2. E.M. Alkoy, M. Papila, Ceram. Int. **36**, 1921–1927 (2010)
3. G. Helke, K. Lubitz, Springer Ser. Mater. Sci. **114**, 89–130 (2008)
4. X. Pang, J. Qiu, K. Zhu, J. Luo, J. Mater. Sci. **46**, 2345–2349 (2011)
5. B. Malic, J. Bernard, J. Holc, D. Jenko, M. Kosec, J. Eur. Ceram. Soc. **25**, 2707–2711 (2005)
6. Y. Guo, K. Kakimoto, H. Ohsato, Appl. Phys. Lett. **85**, 4121–4123 (2004)
7. Y. Saito, H. Takao, T. Tani, T. Nonoyama, K. Takatori, T. Homma, T. Nagoya, M. Nakamura, Nature **432**, 84–87 (2004)
8. F. Rubio-Marcos, P. Ochoa, J. Fernadez, J. Eur. Ceram. Soc. **27**, 4125–4129 (2007)
9. R. Rai, R. Rani, S. Sharma, A.K. Kholkiun, J. Alloy. Compd. **577**, 575–580 (2013)
10. L. Wang, W. Ren, P. Chin Goh, K. Yao, P. Shi, X. Wu, X. Yao, Thin Solid Films **537**, 65–69 (2013)
11. E. Ringgaard, T. Wurlitzer, J. Eur. Ceram. Soc. **25**, 2701–2706 (2005)
12. J. Hao, R. Chu, Z. Xu, G. Zang, G. Li, J. Alloy. Compd. **479**, 376–380 (2009)
13. E. Hollenstein, D. Damjanovic, M. Setter, J. Eur. Ceram. Soc. **27**, 4093–4097 (2007)
14. H. Li, *Thesis Doctoral* (Drexel University, USA, 2008)
15. B. Malic, J. Bernard, A. Bencan, M. Kosec, J. Eur. Ceram. Soc. **28**, 1191–1196 (2008)
16. B. Malic, A. Bencan, T. Rojac, M. Kosec, Acta Chim. Slov. **55**, 719–726 (2008)
17. X. Wang, J. Wun, X. Cheng, B. Zhang, J. Zhu, D. Xiao, Ceram. Int. **39**, 8021–8024 (2013)
18. G. Lévêque, P. Marchet, F. Levassort, L.P. Tran-Huu-Hue, J.R. Duclere, J. Eur. Ceram. Soc. **31**, 577–588 (2011)
19. N. Klein, E. Hollenstein, D. Damjanovic, H.J. Trodahl, N. Setter, M. Kuball, J. Appl. Phys. **102**, 014112 (2007)
20. J. Taub, L. Ramajo, M.S. Castro, Ceram. Int. **39**, 3555–3561 (2012)
21. F. Rubio-Marcos, P. Marchet, T. Merle-Méjean, J.F. Fernandez, Mater. Chem. Phys. **123**, 91–97 (2010)
22. F. Rubio-Marcos, M.G. Navarro-Rojero, J.J. Romero, P. Marchet, J.F. Fernández, IEEE Trans. Ultrason. Ferroelectr. Freq. Control **9**, 1835–1842 (2009)
23. F. Rubio-Marcos, P. Marchet, J.J. Romero, J.F. Fernández, J. Eur. Ceram. Soc. **31**, 2309–2317 (2011)